Structural dynamics of the *Streptomyces lividans* K^+ channel (SKC1): secondary structure characterization from FTIR spectroscopy

Suren A. Tatulian[1], D. Marien Cortes, Eduardo Perozo

Department of Molecular Physiology and Biological Physics, and Center for Structural Biology, University of Virginia Health Sciences Center, P.O. Box 10011, Charlottesville, VA 22906-0011, USA

Received 8 January 1998

Abstract Fourier transform infrared (FTIR) spectroscopy was used to probe the secondary structure, orientation, and the kinetics of amide hydrogen-deuterium exchange (HX) of the small K^+ channel from *Streptomyces lividans*. Frequency component analysis of the amide I band showed that SKC1 is composed of 44–46% α-helix, 21–24% β-sheet, 10–12% turns and 18–20% unordered structures. The order parameter *S* of the helical component of SKC1 was between 0.60 and 0.69. Close to 80% of SKC1 amide protons exchange within ~3 h of D_2O exposure, suggesting that the channel is largely accessible to solvent exchange. These results are consistent with a model of SKC1 in which helices slightly tilted from the membrane normal line the water-filled vestibules that flank the K^+ selectivity filter.

Key words: Channel vestibule; Fourier transform infrared spectroscopy; Hydrogen-deuterium exchange; Potassium channel; *Streptomyces lividans*

1. Introduction

K^+ channels are a widely distributed class of membrane proteins involved in such basic cellular functions as the regulation of electrical activity, signal transduction and osmotic balance. Although gated by an array of different mechanisms, it is apparent that all K^+ channels conform to a common architectural motif in which multiple transmembrane segments are arranged as α-helical bundles [1], and these bundles associate to form oligomers with fourfold symmetry [2,3]. The most remarkable property of the K^+ channel family is perhaps the presence of a common 'signature sequence' or P-loop that is thought to line the pore and forms the K^+ selectivity filter [4–7]. This segment is highly conserved among members of the K^+ channel family and has been used recently to identify potassium channel genes from several genome sequencing projects [8,9].

Schrempf et al. [10] have reported the identification, cloning, expression and single channel characterization of a 160 amino acid potassium channel from the genome of the Gram-positive bacterium *Streptomyces lividans*. The *Streptomyces* K^+ channel (SKC1) is the smallest potassium-selective channel reported so far, and therefore constitutes an appealing target for structural studies. SKC1 contains a canonical P-segment (with 64% identity to the Shaker P-loop), flanked by two putative transmembrane segments (Fig. 1A,B). Recent biochemical studies [11,12] have clearly shown that this channel forms tetramers in detergent, while exhibiting an unusually high oligomeric stability. Initial estimation of its secondary structure from circular dichroism (CD) spectroscopy indicated that SKC1 is mostly α-helical both in detergent and reconstituted in liposomes [11].

Here we have used transmission and polarized attenuated total reflection (ATR) Fourier transform infrared (FTIR) spectroscopy to study the secondary structure of reconstituted SKC1, the orientation of its helical component, and the kinetics of amide hydrogen-deuterium exchange (HX) in supported bilayers. Our results are consistent with the notion that K^+ channels are formed by the oligomerization of bundles of α-helices lining water-filled vestibules flanking the selectivity filter.

2. Materials and methods

2.1. Expression, purification and reconstitution of SKC1

SKC1 was expressed and purified as described [11]. The channel was mixed with detergent-solubilized asolectin and reconstituted by dilution in PBS, this mixture was centrifuged at $100\,000 \times g$ for 1 h, and the pellet resuspended in 1 ml PBS.

2.2. Planar lipid bilayer experiments

Reconstituted SKC1 channels were incorporated into asolectin planar lipid bilayers formed according to the method of Mueller and Rudin [13] using a 20 mg/ml solution of asolectin in decane. Recordings were performed using a home-made current to voltage converter, the data filtered at 1 kHz and stored on a VCR tape for off-line analysis.

2.3. Infrared spectroscopy

ATR FTIR spectra were measured on a Nicolet 740 infrared spectrometer. The spectra of SKC1 solubilized in detergent or reconstituted in phospholipid vesicles were measured in an FTIR precision liquid cell, using CaF_2 windows and 25 μm Teflon spacers (Buck Scientific, East Norwalk, CT). Supported lipid bilayers for the ATR FTIR experiments were prepared as described elsewhere [14]. Proteoliposomes of asolectin with reconstituted SKC1 in H_2O buffer (150 mM NaCl, 10 mM NaPi, pH 7.4) were injected into the ATR cell containing a germanium plate with DPPC monolayers at both surfaces and allowed to spread on the monolayer to yield supported bilayers. Then the cell was flushed with the same buffer to remove excessive vesicles and ATR spectra of SKC1 reconstituted in supported bilayers in H_2O environment were recorded. This was followed by flushing the cell with 10–12 volumes of D_2O buffer (150 mM NaCl, 10 mM Tris, pH* 7.0). In amide HX experiments, the time point of injection of the D_2O buffer was taken as the zero time of exchange. A spectrum was recorded immediately after injection of D_2O buffer, followed by recording of successive spectra with a periodicity of 32 min. All experiments were carried out at ambient temperature.

Curve-fitting of the amide I bands was performed based on the frequencies of the five components of the second derivative spectra; the three central frequencies were fixed while the two bordering fre-

[1]Corresponding authors. Fax: (1) (804) 982-1616.
E-mail: eperozo@virginia.edu; st8m@virginia.edu

Abbreviations: ATR, attenuated total reflection; CD, circular dichroism; DDM, dodecyl maltoside; DPPC, dipalmitoyl phosphatidylcholine; FTIR, Fourier transformed infrared; HX, hydrogen exchange; SKC1, *Streptomyces lividans* small K^+ channel; PBS, phosphate buffered saline

PII S0014-5793(98)00091-X

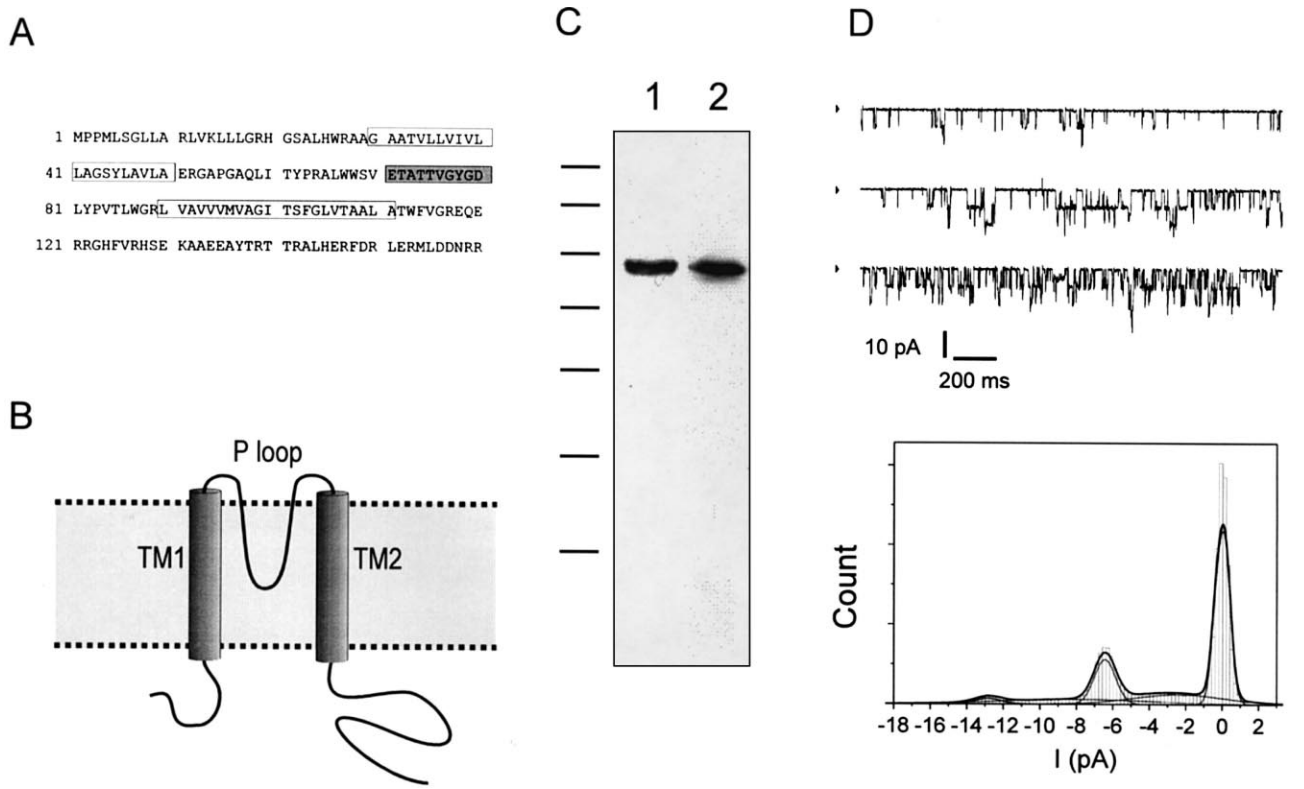

Fig. 1. Biochemical and functional properties of SKC1. A: Deduced amino acid sequence. The open boxes represent the extension of the putative transmembrane helices, and the shaded region identifies the highly conserved P-segment. B: Cartoon of the predicted transmembrane topology for SKC1. C: SDS-PAGE analysis of purified SKC1 in dodecyl maltoside (lane 1) and after reconstitution in asolectin liposomes (lane 2). D: Single channel traces form SKC1 channels reconstituted into planar lipid bilayers. Top, traces obtained at −60 mV in symmetrical 150 mM K_2SO_4, arrows point to the zero current level. Bottom, all-point histogram from the same data. Peaks have been fitted to a sum of Gaussian components assuming that the bilayer contained two channels having a single channel current of 6.4 pA and a subconductance level with a current of 3.1 pA.

quencies were allowed to float. The lineshape of all components was Gaussian.

2.4. Processing of amide hydrogen exchange data

We employed two approaches to evaluate the kinetics of the amide HX and fractions of residues involved in kinetically distinct populations based on time-resolved FTIR spectra of SKC1 reconstituted in supported membranes. In both cases, the time dependence of the fraction of non-exchanged amide hydrogens was expressed as:

$$\left[\frac{\mathrm{H}}{\mathrm{H+D}}\right]_t = a_1 e^{-t/\tau_1} + a_2 e^{-t/\tau_2} + a_3 \quad (1)$$

where a_1, a_2 and a_3 are the fractions of fast exchanging, slow exchanging, and stable residues, respectively, and τ_1 and τ_2 are the time constants of fast and slow exchanging amide hydrogens, respectively. In the first method, the ratio of the integrated areas of amide II ($\sim$1545 cm^{-1}) and amide I ($\sim$1655 cm^{-1}) absorbance bands at time point t, normalized with respect to that ratio at time $\leq$0 (i.e. in H_2O), was used as the fraction of non-exchanged hydrogens:

$$\left[\frac{\mathrm{H}}{\mathrm{H+D}}\right]_t = \frac{\left(\frac{\mathrm{A_{amide\ II}}}{\mathrm{A_{amide\ I}}}\right)_t}{\left(\frac{\mathrm{A_{amide\ II}}}{\mathrm{A_{amide\ I}}}\right)_0} \quad (2)$$

In the second method, the spectrum of the reconstituted protein in H_2O buffer was subtracted from each subsequent spectrum measured after injection of D_2O buffer. The difference spectrum in the amide I region consists of negative and positive parts. The absolute total areas of the difference spectra at time point t ($|\Delta A|_t$) in the amide I region were converted to the fractions of non-exchanged amide hydrogens by:

$$\left[\frac{\mathrm{H}}{\mathrm{H+D}}\right]_t = 1 - \frac{\left[1 - \left[\frac{\mathrm{H}}{\mathrm{H+D}}\right]_T\right] \times |\Delta A|_t}{|\Delta A|_T} \quad (3)$$

where T stands for a time point corresponding to extensive deuteration (in this study, T = 2920 min), and $[H/(H+D)]_T$ was evaluated by Eq. 2 based on spectral changes in the amide II region at time T. Then the data points evaluated through Eqs. 2 and 3 were plotted against time of deuteration and described by Eq. 1, which yielded two sets of parameters a_1, a_2, a_3, τ_1 and τ_2.

According to current models of protein HX [15,16], each residue can be found in two conformational states; in one of these states the residue cannot undergo hydrogen exchange ($HX_{incompetent}$ state) and the other is the readily exchangeable conformation ($HX_{competent}$ state):

$$\mathrm{HX_{incompetent}} \underset{k_{cl}}{\overset{k_{op}}{\leftrightarrow}} \mathrm{HX_{competent}} \xrightarrow{k_{op}} \mathrm{Exchange} \quad (4)$$

where k_{op} and k_{cl} are the rate constants for opening and closing, respectively, and k_0 is the rate constant for an unordered, solvent-exposed peptide. The overall, experimentally observed HX rate constant is:

$$k_{obs} = \frac{k_{op} k_0}{k_{cl} + k_0} \quad (5)$$

Since in most cases it has been found that $k_{cl} \gg k_0$, Eq. 5 can be rewritten as:

$$k_{obs} = \frac{k_{op}}{k_{cl}} k_0 \quad (6)$$

Hydrogen/deuterium exchange is acid- and base-catalyzed, and k_0 is

determined by:

$$k_0 = k_D[D^+] + k_{OD}[OD^-] \quad (7)$$

where k_D and k_{OD} are the acid- and base-catalyzed rate constants. At 0°C, $k_D = 3.54\ M^{-1}\ min^{-1}$ and $k_{OD} = 3.24 \times 10^{10}\ M^{-1}\ min^{-1}$ and the corresponding activation energies are $\Delta E^{\ddagger}$ (k_D) = 15 kcal/mol and $\Delta E^{\ddagger}$ (k_{OD}) = 2.6 kcal/mol [17–19]. Using these values, along with the dissociation constant of D_2O, $K_W(D_2O) = 10^{-15.962}$ [19] and neglecting the effect of side chains [20], we find by Eq. 7 that at 20°C and pH* 7.0 (pD 7.4): $k_0 = 123.1\ min^{-1}$. This corresponds to an exchange reaction with a time constant of ~0.5 s. Now we can evaluate the Gibbs free energy of dynamic opening to hydrogen exchange based on k_0 and the measured rate constant, k_{obs} [15]:

$$\Delta G_{HX} = -RT\ln(k_{obs}/k_0) \quad (8)$$

2.5. Order parameters and protein-to-lipid ratio

Order parameters for proteins and lipids in oriented bilayers are defined as:

$$S = (3\langle\cos^2\theta\rangle - 1)/2 \quad (9)$$

where θ is the angle between the molecular axis and the membrane normal and the angular brackets indicate space- and time-averaging. The order parameters were determined based on measured ATR dichroic ratios as described in Tamm and Tatulian [21].

3. Results

3.1. SKC1 purification and reconstitution

SKC1 was purified as a SDS-insensitive tetrameric complex running anomalously as a single 64 kDa band (Fig. 1C), as reported previously [11,12]. Channels reconstituted in asolectin liposomes by the dilution method were tested functionally after incorporation into planar lipid bilayers. Fig. 1D displays a typical series of single channel recordings obtained from such reconstituted preparations. In agreement with Schrempf et al. [10], we observe two distinct conductance states: in symmetrical 150 mM K_2SO_4 solutions we find a main conductance state at ~140 and a subconductance state close to 75 pS. The 140 pS state was most frequently observed. This purified preparation was subsequently used in all FTIR measurements.

3.2. Secondary structure of SKC1

In Fig. 2A, the infrared absorbance spectra of SKC1 reconstituted in supported bilayers, phospholipid vesicles, and solubilized in 1 mM DDM are shown in the protein amide I (~1655 cm^{-1}) and lipid carbonyl stretching vibrational regions (~1736 cm^{-1}). The peak frequency of the amide I band at ~1655 cm^{-1} indicates high α-helical content in the protein in all three cases [22,23], while the shoulder at 1620–1640 cm^{-1} suggests the presence of considerable fractions of β-structures and/or irregular components in SKC1. Analysis of the corresponding second derivative spectra of SKC1 presented in Fig. 2B reveals the components of the complex amide I and lipid carbonyl bands. The most prominent

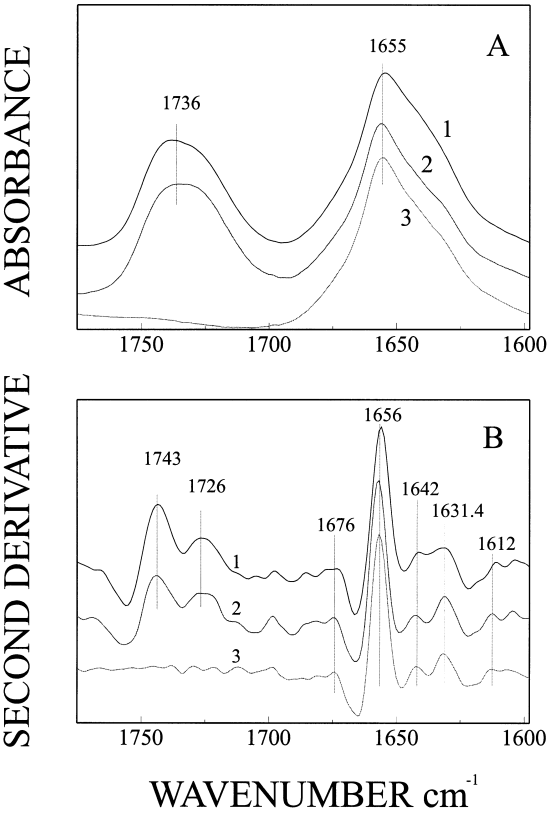

Fig. 2. A: The infrared absorbance spectra of SKC1 reconstituted in DPPC/asolectin supported bilayers, phospholipid (asolectin) vesicles, and solubilized in 1 mM dodecyl maltoside, in the protein amide I and lipid carbonyl stretching vibrational region (curves 1, 2, 3, respectively). The spectrum 1 was recorded using parallel polarized IR light, while the two others were measured using unpolarized light. B: The overturned second derivatives of the curves presented in A. Most prominent peaks in the original and derivative spectra are marked. In all cases, the protein was exposed to D_2O buffer (150 mM NaCl, 10 mM Tris, pH* 7.0) for 2–3 h before recording the spectra.

Table 1
Secondary structure of *Streptomyces lividans* potassium channel in detergent, phospholipid vesicles or substrate-supported bilayers deduced from curve-fitting of amide I infrared absorbance bands[a]

Wavenumber, cm^{-1}	Assignment	Relative content, %		
		Detergent[b]	Vesicles[b]	Supported bilayers[c]
1673.3 ± 0.3	Turn and sheet[d]	11.6 ± 1.0	10.9 ± 1.1	10.3 ± 2.1
1656.2 ± 0.7	α-Helix	44.1 ± 3.8	46.2 ± 2.7	45.7 ± 2.4
1641.8 ± 0.8	Irregular	17.6 ± 4.3	19.6 ± 3.4	18.6 ± 2.0
1631.6 ± 0.6	β-Sheet	23.8 ± 5.7	21.3 ± 3.6	22.8 ± 3.3
1611.0 ± 2.1	Side chains[e]	2.6 ± 1.6	1.9 ± 0.8	2.4 ± 1.2

[a]SKC1 in detergent or phospholipid membranes was exposed to D_2O buffer (150 mM NaCl, 10 mM Tris, pH* 7.0) for several hours before recording the infrared spectra. Therefore the protein should be regarded as partially amide-deuterated.
[b]Spectra of SKC1 in detergent or vesicles were measured by transmission technique.
[c]Spectra of SKC1 in supported bilayers were measured by attenuated total reflection technique.
[d]Antiparallel β-sheets generate split amide I vibrations, one at ~1630 cm^{-1} and two between 1700 and 1666 cm^{-1}.
[e]Protein side chains containing amide groups or aromatic rings generate vibrations at this region.

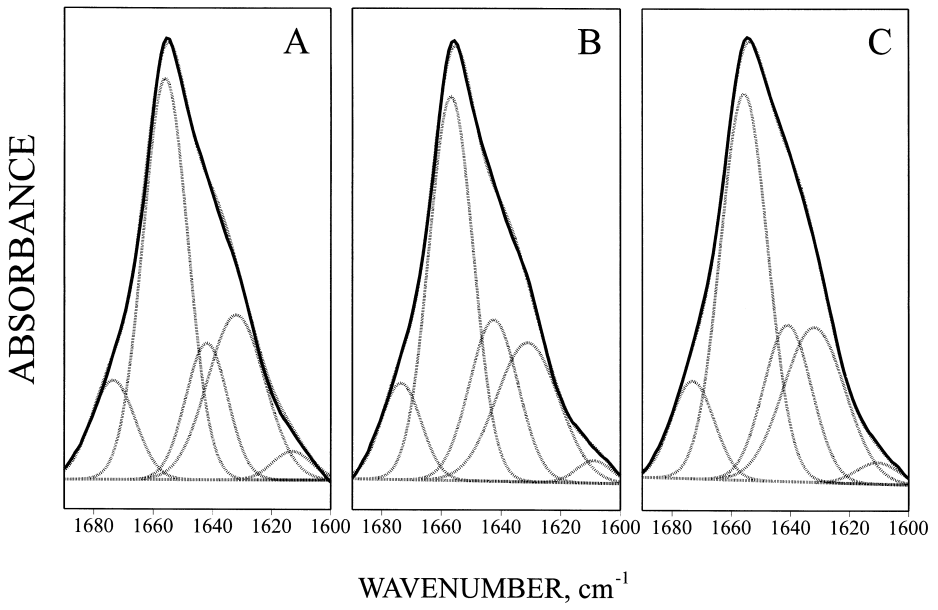

Fig. 3. The results of curve-fitting of the amide I bands of SKC1 solubilized in detergent (A), reconstituted in phospholipid vesicles (B) or supported bilayers (C). The frequencies of the component bands were obtained from the second derivative curves (Fig. 1B) and fixed during the curve-fitting procedure, besides those at ~1673 and ~1611 cm^{-1}, which were not fixed. The amide I bands in A and B were obtained using unpolarized light, and the one in C was recorded with parallel polarized light.

band in the amide I region is centered at 1656 cm^{-1} and corresponds to α-helical secondary structure. Additional amide I components are also identified in the second derivative spectra. Components at ~1642, ~1631, and 1608–1615 cm^{-1} are most likely generated by deuterated irregular structure, β-strands, and side chains, respectively [22–24]. The absorbance in the spectral region 1700–1660 cm^{-1} is generated by the turn structures and the high frequency antiparallel β-sheet counterparts. The absorbance band at ~1736 cm^{-1}, which represents the carbonyl stretching band of the phospholipid, is present in the spectra of SKC1 reconstituted in vesicles or supported membranes and is absent in the spectrum of detergent-solubilized SKC1 (Fig. 2A), a clear indication that 1 mM DDM is enough to completely delipidate the channel. Two components of the lipid carbonyl band at ~1743 and ~1726 cm^{-1} are revealed in the second derivative spectra (Fig. 2B), and are associated with carbonyl groups with different hydration characteristics [25]. The frequencies of the five components of amide I bands, shown in Fig. 2B, were used as input parameters in a curve-fitting program to determine the fractions of corresponding structures in the protein. Results of curve fitting (Fig. 3 and Table 1) demonstrate that the protein is composed of 44–46% α-helix, at least 20% β-strands (to estimate the total fraction of the antiparallel β-sheet, the higher frequency components should be taken into account), 10% turns, and approximately 18% unordered, or irregular structure. Interestingly, the secondary structure composition of SKC1 does not noticeably depend on the type of reconstitution system and is essentially identical in detergent.

3.3. Amide hydrogen exchange

Amide hydrogen exchange experiments were carried out on SKC1 reconstituted in supported membranes to gain additional information on the dynamic structure of this protein, such as the fractions of fast and slow exchanging residues, the corresponding rate constants, and Gibbs free energies of secondary structure chain opening. In the course of amide hydrogen exchange the amide I band shifts to lower frequencies and is significantly reshaped, as shown in the time-resolved spectra of Fig. 4A. The difference spectra in the amide I region, presented in Fig. 4B, illustrate the decrease in absorbance intensity at ~1680 cm^{-1} and increase in absorbance intensity at ~1640 cm^{-1} during deuteration. The intensity of the amide II absorbance band at ~1545 cm^{-1} dramatically decreases because of a ~90 cm^{-1} downshift of this vibrational mode upon amide HX. Both of these effects have been used to quantitatively characterize the amide hydrogen exchange of SKC1, as described in Section 2. The data points of the two curves of Fig. 4C are obtained by Eqs. 2 and 3 based on spectral changes of amide I and amide II bands. The two curves simulated by Eq. 1 yield best fit parameters of $a_1 = 0.406$, $\tau_1 = 1.246$ min, $a_2 = 0.539$, $\tau_2 = 129.4$ min, $a_3 = 0.055$ (based on amide II band area changes) and $a_1 = 0.467$, $\tau_1 = 0.896$ min, $a_2 = 0.436$, $\tau_2 = 165.3$ min,

Table 2
Characterization of structural dynamics of SKC1 by amide hydrogen exchange[a]

	Method 1[b]	Method 2[b]
a_1	0.41	0.47
τ_1 (min)	1.25	0.90
a_2	0.54	0.44
τ_2 (min)	129	165
a_3	0.055	0.096
$\Delta G_{HX,1}$ (kcal/mol)	2.93	2.74
$\Delta G_{HX,2}$ (kcal/mol)	5.63	5.77

[a] a_i are the fractions of residues in ith population, characterized by time constant of hydrogen exchange, τ_i, and free energies of dynamic opening to hydrogen exchange, $\Delta G_{HX,1}$; a_3 is the fraction of stable residues that are well protected from exchange.
[b] Methods 1 and 2 are based on spectral changes in the amide II and amide I regions, respectively (see Section 2).

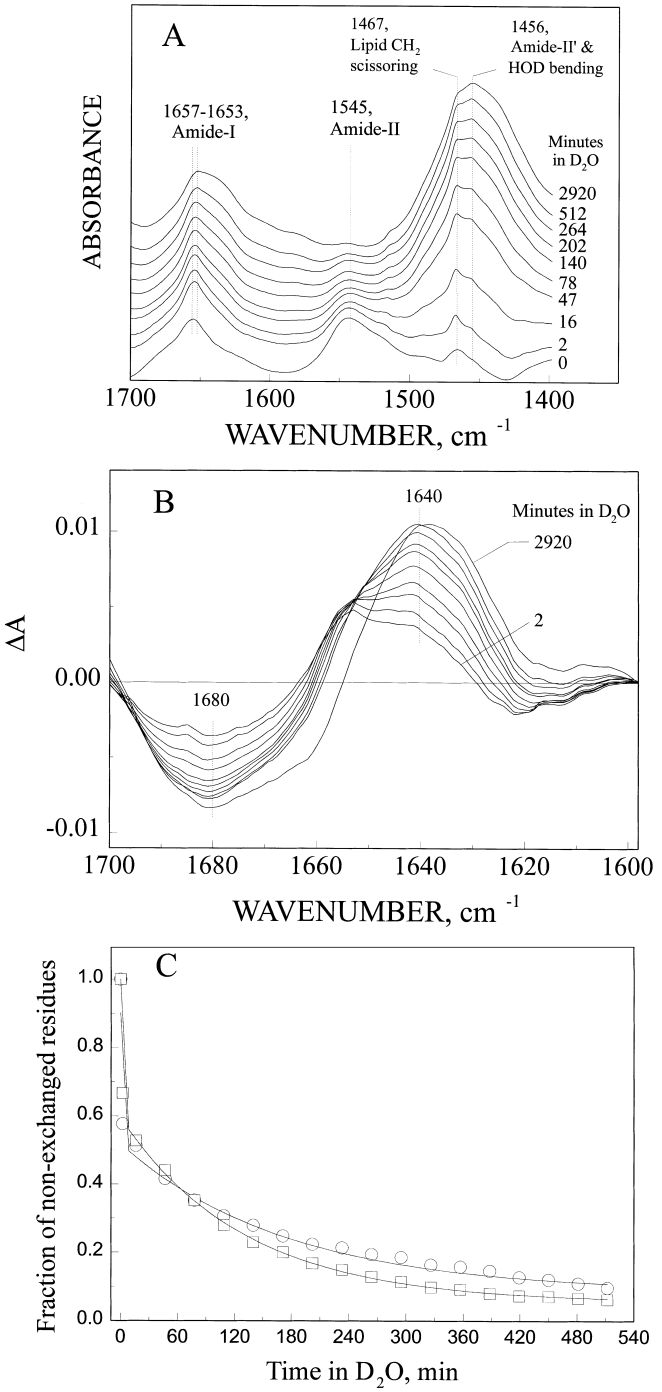

Fig. 4. A: Time-resolved spectral changes in the amide I (I′) and amide II (II′) regions of SKC1 reconstituted in DPPC/asolectin supported bilayers in response to amide H/D exchange. B: Difference spectra reflecting spectral changes in the amide I region in the course of amide H/D exchange of reconstituted SKC1. The difference spectra were obtained by baseline correcting and normalizing the amide I bands and subtracting the spectrum recorded in H_2O buffer from those recorded in D_2O buffer. C: Time dependence of the fraction of non-exchanged protein residues estimated based on the spectral changes in the amide II region (squares) and in the amide I region (circles). The curves were simulated through Eq. 1 using parameters $a_1 = 0.406$, $k_1 = 0.802$ min^{-1}, $a_2 = 0.539$, $k_2 = 0.00773$ min^{-1}, $a_3 = 0.055$ (squares) and $a_1 = 0.467$, $k_1 = 1.116$ min^{-1}, $a_2 = 0.436$, $k_2 = 0.00605$ min^{-1}, $a_3 = 0.096$ (circles).

$a_3 = 0.096$ (based on amide I band transformations). These results show that 41–47% of the backbone amide protons of SKC1 reconstituted in supported bilayers exchange within a time scale of 1 min, 44–54% of residues exchange with a time constant of 2–3 h, and 5–10% of residues are resistant to HX, or exchange with a time constant of $\gg 2$ h. Time constants τ_1 and τ_2 were used to calculate, according to Eq. 8, the Gibbs free energies of the dynamic conformational fluctuations of amide groups in the corresponding kinetic populations. Values of $\Delta G_{HX} \sim 2.7$–2.9 kcal/mol were obtained for fast exchanging amide groups, while the slower exchanging population had values of $\Delta G_{HX} \sim 5.6$–5.8 kcal/mol (see Table 2).

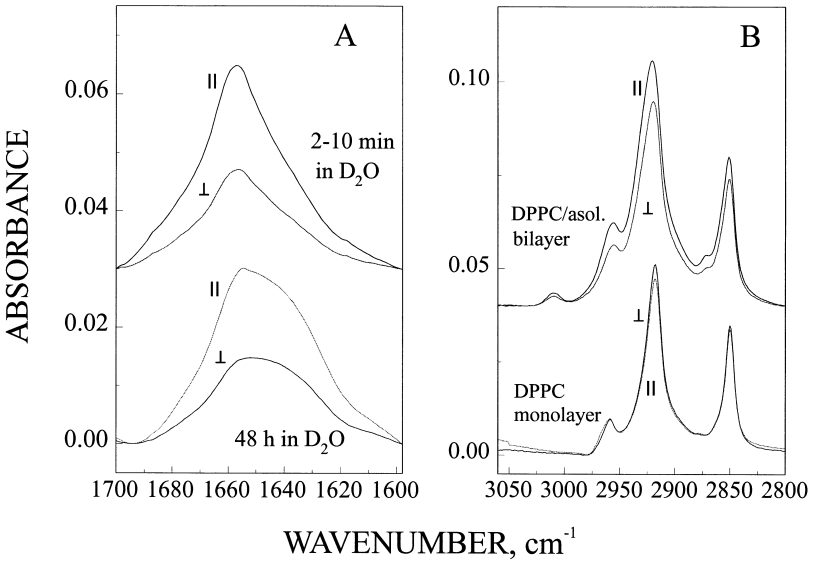

Fig. 5. A: ATR amide I bands of SKC reconstituted in a DPPC/asolectin supported bilayer at parallel and perpendicular polarization of the infrared beam, exposed to D_2O buffer for 2–10 min and for 48 h, as indicated. The order parameter, $S = 0.604$–0.688 was calculated according to Eq. 9, with $\alpha = 39°$ for the amide I transition moment of α-helices [38,39], the fraction of helix in SKC1 $f = 0.45$ (Table 1), and $E_x^2 = 1.9691$, $E_y^2 = 2.2486$, $E_z^2 = 1.8917$. The electric field components were calculated using an incidence angle $\gamma = 45°$ and refractive indices $n_1 = 4$, $n_2 = 1.43$, and $n_3 = 1.33$ [40]. B: Polarized ATR absorbance bands of the lipid CH_2 stretching mode for a DPPC supported monolayer and after formation of a DPPC/asolectin supported bilayer with reconstituted SKC1, as indicated.

3.4. Orientation of SKC1 in supported membranes

The ATR amide I absorbance bands of SKC1 reconstituted in supported bilayers are presented in Fig. 5A at parallel and perpendicular polarizations of the infrared light (both within 2–10 min and after 48 h of H/D exchange). Irrespective of the degree of deuteration, the protein exhibits an ATR dichroic ratio of 2.03–2.08, determined on the basis of peak frequencies or integrated areas of amide I bands. Using these dichroic ratios, the parameters $E_x^2 = 1.969$, $E_y^2 = 2.249$, $E_z^2 = 1.892$, $\alpha = 39°$ [21] and $f = 0.45$ (Table 1), we calculated the orientational order parameter of the helices of SKC1 in supported bilayers as $S = 0.60$–0.69. Assuming that all helices responsible for dichroism are oriented similarly, these values corresponds to an average tilt angle $\theta = 27$–$31°$ from the membrane normal.

It is reasonable to expect a correlation between the order parameters of the transmembrane helices of a reconstituted integral protein and the lipid hydrocarbon chains. The R^{ATR} of the DPPC monolayer, deposited on the germanium plate, was 0.94 (Fig. 5B). Using $n_3 = 1$ for air, which corresponds to $E_z^2 = 0.6046$, we calculate an order parameter $S = 0.68$. The dichroic ratio of the supported bilayer with reconstituted SKC1, after removing the excess vesicles, was 1.28, corresponding to $S = 0.42$ (calculated with $n_3 = 1.33$ and $E_z^2 = 1.8917$ for water). The increased width and slightly higher peak frequencies of lipid CH_2 stretching vibrational bands also indicate a lower order of the lipid in the bilayer than in the monolayer. In spite of a decrease in the lipid order parameter during formation of the bilayer, which presumably results from exposure of the monolayer to an aqueous medium and the presence of unsaturated (less ordered) hydrocarbon chains in asolectin, the lipid is still reasonably well ordered in the supported bilayer.

4. Discussion

We have investigated the secondary structure of SKC1 using transmission and ATR-FTIR spectroscopy in an attempt to determine: (1) the relative proportions of its secondary structure components, (2) the dynamics and solvent accessibility through H/D exchange and (3) the orientation of the channel α-helices with respect to the membrane plane.

Our results clearly indicate that the α-helix is the dominant secondary structure component in SKC1, having approximately 46% of its residues in this conformation. About 33% of the channel adopts β-strand and turn structures and ~18% of the molecule is in irregular conformation (see Table 1). This secondary structure assignment is essentially identical for the three different conditions tested (detergent, liposomes and supported bilayers), a result we have taken as an indication of the structural integrity of the purified protein and one which is consistent with its documented stability in detergent. Nonetheless, we find a quantitative discrepancy in the absolute amount of α-helices reported by FTIR and by CD spectroscopy. While the present results suggest about 46% α-helix content, our previous CD measurements point to 55–59% α-helical content for reconstituted and detergent solubilized SKC1 respectively [11]. In fact, higher quality CD spectra of detergent-solubilized SKC1 obtained at wavelengths down to 180 nm reveal helical contents of 58% (E. Perozo, unpublished results). Lower α-helical estimates from FTIR have been reported in the literature [26,27]. Due to the fact that CD and FTIR are subject to different sources of error, they are considered complementary techniques in the estimation of the secondary structure of proteins [23,27,28]. While β-sheets and irregular structures are more reliably estimated from FTIR spectra, CD spectra are superior in the quantification of α-helices [27,28]. Thus, by combining the strengths of each technique we can suggest that SKC1 is composed of ~55% α-helix, ~30% β-structure and ~15% irregular structures.

The absence of the phospholipid carbonyl stretching band at ~1736 cm^{-1} of SKC1 solubilized at 1 mM dodecyl maltoside (Fig. 2A) directly indicates a complete detergent-mediated

delipidation of the channel and supports the view that SKC1 is stable as a tetramer in the absence of phospholipids. This result is a notable departure from the behavior of other ion-selective channels, like the eel electroplax Na^+ channel [29], or the Drosophila Shaker K^+ channel [30,31] where the stability of the channel in detergent micelles is strictly dependent on the presence of phospholipids.

Data on amide hydrogen exchange contain a wealth of information regarding the solvent accessibility, the strength of hydrogen bonding, and dynamic structure of proteins. Individual amide protons show specific rates of exchange that can correlate with local mobility and structure as well as hydrogen bonding state and steric protection. Protein HX data have been described dividing amide protons into two to four kinetically discrete populations [32–34]. Our HX data suggests that SKC1 residues may be clustered into three populations with distinct secondary, tertiary and quaternary structural features. One population, comprising 41–47% of residues, is characterized by a HX time constant of $\sim$1 min, and a Gibbs energy of opening to HX ΔG_{HX} $\sim$2.8 kcal/mol (Table 2). This value is close to the ΔG of amide hydrogen bonding ($\sim$3.1 kcal/mol in water at 25°C), suggesting that these may be the residues involved in solvent-exposed hydrogen-bonded secondary structures. The residues of interhelical loops, transmembrane helices lining the water pore, and those close to the membrane/water interface, are indeed good candidates for such residues. However, this fast exchanging population is likely to include non-hydrogen-bonded residues that are not kinetically resolved in our experiments. The second population, encompassing 44–54% of residues, has a time constant of 2–3 h, and ΔG_{HX} $\sim$5.7 kcal/mol. The best candidates for the residues in this population are those involved in secondary structures and partially accessible to water, such as lipid-exposed helical residues, and non-hydrogen-bonded residues partially buried in the protein. The third population includes 5–10% of HX-resistant residues and may comprise the residues of transmembrane helices at interhelical interfaces completely buried in the protein core. For comparison, H/D exchange studies in bacteriorhodopsin, where most of the transmembrane segments are buried in the membrane, reveal that more than 70% of the amide I protons remain unexchanged after 48 h of incubation in D_2O [35]. The fact that only 20% of the amide I protons are protected from exchange within $\sim$3 h is not surprising, if we consider that SKC1 possesses a water-filled ion pore. As suggested for other K^+ channels, this pore communicates to the bulk solution through intra- and extracellular 'vestibules', which will likely contribute to the solvent accessible area of SKC1. In fact, a correlation between high efficiency of HX and the presence of water-filled pores or cavities have been suggested for other transport proteins like the erythrocyte glucose transporter [36] and the erythrocyte water channel aquaporin I [37].

We determined the molecular orientation in supported bilayers by polarized ATR FTIR spectroscopy using an angle $\alpha = 39°$ for the amide I transition moment [38,39]. We also ascribed the dichroism of the amide I band to the helices of the reconstituted protein, and suggested that the helices are oriented similarly. This approach yielded an order parameter $S = 0.60–0.69$, values that correspond to a tilt angle $\theta = 27–31°$ relative to the membrane normal. Considering the non-ideal surface flatness of the substrate and that the measured R^{ATR} (which we attribute to transmembrane α-helices) could be contaminated by other helical or non-helical structures, our estimate of the helical order parameter is likely to be lower than its actual value. For example, our initial secondary structure predictions [11] have indicated potential helical segments in both the N- and C-termini of the channel. Some of these helices are clearly amphipathic and could sit parallel to the plane of the membrane, thus producing an underestimation of the order parameter of membrane-spanning helices.

Current views on potassium channel architecture suggest that these membrane proteins are homo-tetramers formed by the association of helical bundles with fourfold symmetry around the potassium ion pathway [1]. Under this arrangement, intra- and extracellular vestibules flank the narrow portion of the aqueous pore (the selectivity filter). The present results tend to support this type of model in the case of SKC1, and by extension, for the general case of eukaryotic inward-rectifier K^+ channels whose topologies also include a P-loop segment with two-transmembrane helices.

Acknowledgements: The authors are grateful to Dr. Gabor Szabo for the use of his bilayer set-up. Dr. Lukas Tamm critically read the manuscript. This work was supported by USPHS Grant GM RO154690 to E.P. and AHA Grant 96-1364 to S.A.T.

References

[1] Jan, L.Y. and Jan, Y.N. (1994) Nature 371, 119–122.
[2] MacKinnon, R. (1991) Nature 350, 232–235.
[3] Li, M., Unwin, N., Stauffer, K.A., Jan, Y.N. and Jan, L.Y. (1994) Curr. Biol. 4, 110–115.
[4] Hartmann, H.A., Kirsch, G.E., Drewe, J.A., Taglialatela, M., Joho, R.H. and Brown, A.M. (1991) Science 251, 942–944.
[5] Heginbotham, L., Abramson, T. and MacKinnon, R. (1992) Science 258, 1152–1155.
[6] Heginbotham, L., Lu, Z., Abramson, T. and MacKinnon, R. (1994) Biophys. J. 66, 1061–1067.
[7] Yellen, G., Jurman, M.E., Abramson, T. and MacKinnon, R. (1991) Science 251, 939–942.
[8] Ketchum, K., Klenk, H.-P., White, O. and Venter, J.C. (1997) Biophys. J. 72, a354.
[9] Clayton, R.A., White, O., Ketchum, K.A. and Venter, J.C. (1997) Nature 387, 459–462.
[10] Schrempf, H., Schmidt, O., Kummerlen, R., Hinnah, S., Muller, D., Betzler, M., Steinkamp, T. and Wagner, R. (1995) EMBO J. 14, 5170–5178.
[11] Cortes, D.M. and Perozo, E. (1997) Biochemistry 36, 10343–10352.
[12] Heginbotham, L., Odessey, E. and Miller, C. (1997) Biochemistry 36, 10335–10342.
[13] Mueller, P., Rudin, D.O., Tien, H. and Wescott, W.C. (1962) Nature 194, 979–980.
[14] Tatulian, S.A., Jones, L.R., Reddy, L.G., Stokes, D.L. and Tamm, L.K. (1995) Biochemistry 34, 4448–4456.
[15] Bai, Y., Englander, J.J., Mayne, L., Milne, J.S. and Englander, S.W. (1995) Methods Enzymol. 259, 344–356.
[16] Miller, D.W. and Dill, K.A. (1995) Protein Sci. 4, 1860–1873.
[17] Englander, S.W. and Poulsen, A. (1969) Biopolymers 7, 379–393.
[18] Roder, H., Wagner, G. and Wuthrich, K. (1985) Biochemistry 24, 7407–7411.
[19] Robertson, A.D. and Baldwin, R.L. (1991) Biochemistry 30, 9907–9914.
[20] Molday, R.S., Englander, S.W. and Kallen, R.G. (1972) Biochemistry 11, 150–158.
[21] Tamm, L.K. and Tatulian, S.A. (1993) Biochemistry 32, 7720–7726.
[22] Krimm, S. and Bandekar, J. (1986) Adv. Protein Chem. 38, 181–364.
[23] Surewicz, W.K., Mantsch, H.H. and Chapman, D. (1993) Biochemistry 32, 389–394.

[24] Jackson, M. and Mantsch, H.H. (1995) Crit. Rev. Biochem. Mol. Biol. 30, 95–120.
[25] Blume, A., Hubner, W. and Messner, G. (1988) Biochemistry 27, 8239–8249.
[26] Van Hoek, A.N., Wiener, M., Bicknese, S., Miercke, L., Biwersi, J. and Verkman, A.S. (1993) Biochemistry 32, 11847–11856.
[27] Baumruk, V., Pancoska, P. and Keiderling, T.A. (1996) J. Mol. Biol. 259, 774–791.
[28] Pribic, R., van Stokkum, I.H., Chapman, D., Haris, P.I. and Bloemendal, M. (1993) Anal. Biochem. 214, 366–378.
[29] Agnew, W.S. and Raftery, M.A. (1979) Biochemistry 18, 1912–1919.
[30] Sun, T., Naini, A.A. and Miller, C. (1994) Biochemistry 33, 9992–9999.
[31] Cuello, L.G. and Perozo, E. (1997) Biophys. J. 72, a350.
[32] Heimburg, T. and Marsh, D. (1993) Biophys. J. 65, 2408–2417.
[33] Kim, K.S., Fuchs, J.A. and Woodward, C.K. (1993) Biochemistry 32, 9600–9608.
[34] Raussens, V., Narayanaswami, V., Goormaghtigh, E., Ryan, R.O. and Ruysschaert, J.M. (1996) J. Biol. Chem. 271, 23089–23095.
[35] Earnest, T.N., Herzfeld, J. and Rothschild, K.J. (1990) Biophys. J. 58, 1539–1546.
[36] Alvarez, J., Lee, D.C., Baldwin, S.A. and Chapman, D. (1987) J. Biol. Chem. 262, 3502–3509.
[37] Haris, P.I., Chapman, D. and Benga, G. (1995) Eur. J. Biochem. 233, 659–664.
[38] Bradbury, E., Brown, L., Downie, A., Elliott, A., Fraser, R. and Hanby, W. (1962) J. Mol. Biol. 5, 230–247.
[39] Tsuboi, M. (1962) J. Polymer Sci. 59, 139–153.
[40] Fringeli, U. (1993) in: Internal Reflection Spectroscopy: Theory and Applications (Mirabella, F.J., Ed.), pp. 255–324, Marcel Dekker, New York.